Effect of Viscoelastic Interfaces on Thermo-Mechanical Behavior of a Layered Functionally Graded Spherical Vessel

A. Talezadehlari[1], A. Nikbakht[2*], M. Sadighi[3], H. Yademellat[2]

[1] Mechanical Engineering Department, University of Larestan, Lar, Iran

[2] New Technologies Research Center (NTRC), Amirkabir University of Technology, Tehran, Iran

[3] Department of Mechanical Engineering, Amirkabir University of Technology, Tehran, Iran

ABSTRACT: In layered structures, the interface of layers is not always perfect and the analysis of problems which have imperfect interfaces is of the high level of importance. In this paper, an analytical approach is used to study the behavior of a layered functionally graded spherical vessel under thermal and mechanical loadings at the inner and outer surfaces. The interfaces of the layers in the vessel are considered to be imperfect and a viscoelastic layer of negligible thickness is assumed between any two layers. The behavior of these viscoelastic layers is modeled by means of Kelvin-Voigt model. In order to solve the problem, the governing equations of each layer are extracted via the thermoelasticity theory and by applying the appropriate boundary conditions at the interface of the layers, the overall displacement and stress fields are found in the vessel and numerical results are presented for different parameters. The obtained results show that the stiffness of the viscoelastic layer affects the value of the displacements and the stresses as well as the stabilization time of the system. However, changing the damping parameter of the Kelvin-Voigt model only changes the stabilization time and not the values of the displacements and stresses.

1- Introduction

Spherical vessels are one of the most widely used structures in a variety of industries, where these structures, depending on their function, are subjected to different types of loadings. . On the other hand, one way to improve the structural thermo-mechanical behavior of the spherical vessels is to take advantage of the concept of layer-wise Functionally Graded Materials (FGMs); where the combination of the FGMs excellent endurance against thermal and mechanical loadings and the simplicity of the layered structures, turns the resulted structure into an exceptional one.

Regarding this fact, many researchers have focused on the thermo-mechanical behavior of these structures and also the impact of various parameters on their behavior. Noda [1] has investigated the thermal stresses in the temperature-dependent materials. Lutz and Zimmerman [2] have presented an exact solution for a uniform heated spherical object whose elastic modulus and heat conduction coefficient vary linearly with radius. By employing the infinitesimal theory of elasticity, Tutuncu and Ozturk [3] have presented the closed-form solutions for stresses and displacements in functionally graded cylindrical and spherical vessels which are subjected to internal pressure. You et al. [4] have investigated the internally pressurized thick-walled spherical pressure vessels, using elastic analysis. In their work, two kinds of pressure vessels have been considered; one consists of two homogeneous layers at the inner and outer surfaces of the

vessel connected with a functionally graded layer, while the other consists of only the functionally graded material. In their study, they have proposed a method to obtain an almost constant circumferential stress in the vessels consisting of functionally graded materials. Eslami et al. [5] have presented an analytical general solution for the one-dimensional steady-state thermal and mechanical stresses in thick-walled spheres made of functionally graded materials. Poultangari et al. [6] have developed an analytical method to obtain the two-dimensional steady-state thermal and mechanical stresses in FG thick-walled spheres. Akis [7] has investigated the purely elastic, partially plastic and fully plastic stress states in internally pressurized functionally graded spherical pressure vessels in the framework of small deformation theory; where the basis of the plastic model is considered to be Tresca's yield criterion and ideal plastic material behavior. Tutuncu and Temel [8] determined the axisymmetric displacements and stresses in functionally graded hollow cylinders, disks, and spheres subjected to uniform internal pressure by means of plane elasticity theory and complementary functions method. In their research, arbitrary material properties distribution is assumed. This assumption yields a two-point boundary value problem with a governing differential equation of variable coefficients. General analytical solutions of such equations are not available; however, the employed complementary functions method reduces the boundary value problem to an initial value problem which can accurately be solved by one of many efficient methods, such as the Runge-Kutta method. Jabbari et al. [9] have presented a general solution for one-dimensional steady-state thermal and mechanical stresses in

Corresponding author, E–mail: anikbakht@aut.ac.ir

a hollow thick-walled porous FG sphere which is subjected to thermal and mechanical boundary conditions on the inner and outer surfaces and an arbitrary radial temperature function. Nejad et al. [10] have presented exact closed-form solutions for stresses and the displacements in thick-walled FG spherical shells. In their paper, they have analyzed the same problem by means of finite element method as well. Bayat et al. [11] have studied a thermo-mechanical elasticity problem of an FG hollow sphere subjected to mechanical loads and one-dimensional steady-state heat transfer. They implemented the effect of material properties distribution in the sphere by assigning a dimensionless parameter, whose value characterizes the non-homogeneity.

As can be seen, the analytical determination of displacement and stress fields in FG and layered spheres has been widely studied in the literature. However, one of the most important points that must be considered in the analysis of these structures is the perfectness of the bonding between different layers. This fact has categorized the problems of this kind into problems with perfect and imperfect interfaces. If the bonding of the layers is considered to be perfect and flawless, the displacement field is continuous throughout the medium as well as the interfaces. This assumption simplifies the governing equations and enables the researchers to obtain analytical solutions for the stress and displacement fields. Nevertheless, in functional and actual structures, perfect bonding of layers is almost not attainable due to manufacturing processes. The behavior of these kinds of interfaces that are called imperfect interfaces should be considered in the displacement and stress analysis of the FG medium, since in these problems the displacement field will no longer be continuous at the interfaces. There are a number of models which take into account the presence of these discontinuities into the formulation of the governing equations by considering an interlayer of negligible thickness among other layers of the structure. One of the simplest models in determining the behavior of this interlayer is the linear spring model that is used widely by many researchers. In this model, the interlayer is simulated as a spring whose displacement is directly relevant to its applied load by a stiffness factor of that layer. Another model that is also used is the viscose model in which the interlayer is considered as a damper. This means that even under static loads, the response of the structure will be time-dependent [12-18]. The third approach is to consider the interlayer as a viscoelastic layer whose behavior is a combination of the two previously mentioned models. The viscoelastic model can also be utilized in modeling the high-temperature loading conditions. Thus, the viscoelastic model may be used in investigating creep and stress relaxation problems [19, 20].

In all of the above-mentioned studies, the bonding between the layers is assumed to be perfect and flawless. However, some researchers have studied imperfect bonding of layers, as well. Hen and Jiang [21] have studied the time-dependent response of a simply supported layered FG strip with the viscoelastic interface of layers under bending. Their results showed that the behavior of the structure is significantly time-dependent. Chen and Lee [22] have presented a semi-analytical solution to study simply supported composite laminates with viscous interfaces. Based on the findings of this research, as the time approaches infinity, the viscous layer completely loses its ability to transfer shear stress. Yan and Chen [23] have analyzed the same structure but with considering viscoelastic rather than viscous interfaces. They have utilized the Kelvin–Voigt relation to characterize the constitutive behavior of the interfaces. Their findings showed that unlike the viscous interfaces, viscoelastic interfaces can transfer the shear stresses even when the time approaches infinity. The model proposed by He and Jiang [21] is similar to the method presented by Pagano et al. [24-26] for laminated composite and sandwich beams and plates, where He and Jiang [21] have extended the mentioned method by adding an extra step to solve a first-order ordinary differential equation which describes the time-dependent behavior of the interfacial sliding displacement of the iscoelastic interfaces. However, He and Jiang's method, as well as Pagano's solution, needs a large amount of computational capacity when the number of layers is increased. In order to overcome this dilemma, Chen et al. [27] employed the state-space solution technique, with a combination of power series expansion method. They studied the response of a simply supported orthotropic laminate with viscous interfaces. Chen et al. [28] also investigated the same structure by means of state-space and Taylor series expansion methods. By improving and extending the Chen and Lee's method [22], Chen et al. [29] investigated the three-dimensional bending problem of a simply supported cross-ply cylindrical laminate with viscous interfaces. The time-dependent behavior of a simply supported laminated beam, containing two piezoelectric layers at the upper and lower surfaces, has been studied by Yan et al. [30-31], where state space has been employed. In this problem, the piezoelectric layers are attached to the beam by means of viscoelastic interfaces whose behavior is characterized by the Kelvin-Voigt relation. Yan and Chen [32] examined the same problem, but instead of the laminated beam, a functionally graded beam was considered. Wei et al. [33] have analyzed the three-dimensional bending problem of an orthotropic laminated plate with viscoelastic interfaces by using power series expansion and by considering the Kelvin-Voigt viscoelastic relation for the behavior of the interfaces. Yan et al. [34] have investigated the response of a simply supported cross-ply plate with viscoelastic interfaces, subjected to sinusoidal loading. In their study, a comprehensive comparison is made between the behavior of two structures with perfect and imperfect interfaces. Yan et al. [35] have studied the time-dependent bending response of a laminate plate which consists of piezoelectric layers with viscoelastic interfaces. Alibeigloo [36] has studied the bending and free vibration behavior of a simply supported cylindrical panel consisting of homogeneous layers which are connected with viscoelastic interfaces. In this study, the Fourier series are utilized along the axial and circumferential directions and state space technique is used in the radial direction. Alibeigloo [37] has also investigated the three-dimensional static and vibration behavior of a laminated composite plate with viscoelastic interfaces under bending.

As reviewed above, the imperfect bonding between the layers is studied mostly in layered and graded beams and plates while there are few investigations conducted on the behavior of layered and graded cylindrical and spherical structures with imperfect bonding. However, these two latter are among the most important structures in industrial and practical applications, since all pressure vessels are produced in the form of cylindrical or spherical structures. Therefore, a

thorough study of the thermo-mechanical elasticity problem of such structures is needed in order to provide engineers with basic design tools.

In this paper, the steady-state thermo-mechanical elasticity problem of a functionally graded layered spherical pressure vessel with the imperfect bonding of layers is studied. The most general case is considered, where the material properties of each layer are assumed to be constant and the non-homogeneity concept accompanied with functionally graded materials is implied via changing the material properties of each layer gradually in the radial direction. The bonding of the layers is assumed to be viscoelastic and the Kelvin-Voigt model is considered to define the interfacial behavior. If the bonding of the layers is assumed to be perfect, the problem reduces to the thermo-mechanical elasticity problem of a functionally graded sphere. In order to solve the problem, the sphere is considered to be initially under a constant heat flux at its inner surface. After the stabilization of the temperature gradient, mechanical pressure is applied to the inner and outer surfaces of the vessel. Therefore, in the first step of analyzing the problem, the temperature gradient is determined by solving the heat conduction equation and the displacement and stress fields are calculated according to this temperature gradient. Subsequently, the displacement and stress fields due to the mechanical loading are determined, and by using the superposing principle, total displacement and stress fields are found. In each step, the problem is solved analytically by solving the governing equations for each layer and applying the viscoelastic behavior of the interfaces as the boundary conditions. The effects of different parameters, such as time, mechanical pressure, thermal loading and viscoelastic parameters on the response of the vessel are studied by this method.

2- Solution method

The main goal of this research is to present a theoretical approach to investigate the behavior of a layered spherical vessel with viscoelastic interfaces between the layers, subjected to the thermo-mechanical loading. Each layer is assumed to be homogeneous and isotropic and the viscoelastic interfaces are modeled by the Kelvin-Voigt method. Convection heat transfer at the inner and outer surfaces is considered as the thermal boundary conditions of the problem. By assuming infinite heat transfer coefficient, the constant temperature boundary conditions can be achieved, as well. The schematic of the problem geometry is demonstrated in Fig. 1, where the vessel is divided into N layers and E_j, α_j, k_j, h_j and r_j are the modulus of elasticity, coefficient of thermal expansion, thermal conductivity, thickness and the local radial coordinate of the j-th layer ($j=1,\ldots,N$), respectively. In addition, P_{in} and P_{out}, h_{in} and h_{out}, $T_{\infty,in}$ and $T_{\infty,out}$ denote the inner and outer pressure, convection heat transfer coefficient and temperature.

In order to analyze the problem, it is assumed that the vessel is initially subjected to the thermal loading and after the stabilization of the thermal gradient, the mechanical pressure is applied. In order to do so and as the first stage, convection heat transfer is considered at the inner and outer surfaces of the vessel as the thermal boundary conditions and by solving one-dimensional heat conduction equation, the temperature gradient is obtained through the thickness of the vessel. Then, by solving the equilibrium equations and
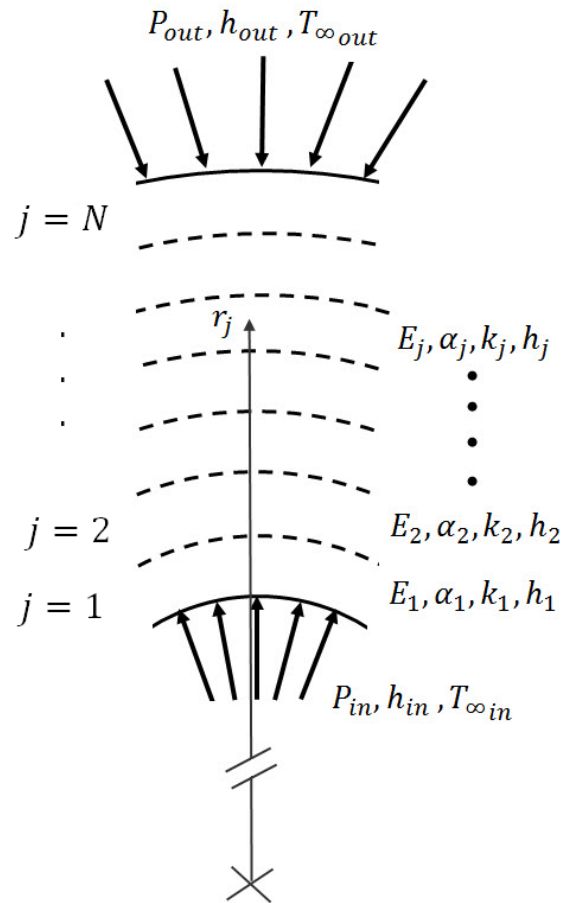
Fig. 1. The schematic of vessel geometry and the applied mechanical and thermal loads

considering the viscoelastic interfaces, this gradient is related to the displacement and stress fields. In the second step, the displacement and stress fields due to the internal pressure are obtained by solving the equations of equilibrium for each layer and applying the continuity boundary conditions at the interfaces of layers. The total displacement and stress fields are derived by means of the superposition principle.

2- 1- Thermal loading

Since the geometry is considered to be spherical and due to the symmetry, $\partial/\partial\varphi$ and $\partial/\partial\theta$ vanish in the equations and the heat conduction equation for each layer in the steady-state is written as:

$$\frac{1}{r_j^2}\frac{d}{dr_j}\left(k_j r_j^2 \frac{dT^j}{dr_j}\right)=0, \quad j=1,\ldots,N \tag{1}$$

In this equation, $T^j=T^j(r_j)$ is the temperature at the j-th layer. Since each layer is considered to be homogeneous, the solution of Eq. (1) may be written as:

$$T^j=\frac{D_1^j}{r_j}+D_2^j, \quad j=1,\ldots,N \tag{2}$$

where D_1^j and D_2^j ($j=1,\ldots,N$) are unknown coefficients obtained by applying the boundary conditions. In the present problem, the boundary conditions are the continuity of temperature and heat flux at the interfaces of the layers:

$$T^j\big|_{r_{j+1}} = T^{j+1}\big|_{r_{j+1}}, \quad j=1,\ldots,N-1 \tag{3a}$$

$$k_j \frac{dT^j}{dr_j}\bigg|_{r_{j+1}} = k_{j+1} \frac{dT^{j+1}}{dr_{j+1}}\bigg|_{r_{j+1}}, \quad j=1,\ldots,N-1 \tag{3b}$$

Furthermore, at the inner and outer surfaces of the vessel convection, heat transfer occurs with the ambient. Therefore, the thermal boundary conditions at the inner and outer surfaces can be written as:

$$h_{in}\left(T_{\infty in} - T^1(r_{in})\right) = -k_1 \frac{dT^1}{dr_1}(r_{in}) \tag{4}$$

$$h_{out}\left(-T^N(r_{out}) - T_{\infty out}\right) = -k_N \frac{dT^N}{dr_N}(r_{out}) \tag{5}$$

In a general case, this problem contains two unknown coefficients in each layer, D_1^j and D_2^j (j=1,…,N); thus, for a structure with N layers, there will be $2N$ unknown coefficients at hand. On the other hand, repeating Eqs. (3a) and (3b) for (N-1) number of interfaces plus Eqs. (4) and (5), result in $2N$ equations. These $2N$ equations and $2N$ unknowns form a linear set of equations whose solution gives D_1^j and D_2^j (j=1,…,N) for all layers.

At the next step, by using the obtained temperature distribution from the previous step, the displacement and thermal stress fields may be determined. Due to the symmetry in both geometry and loading, the parameters will not change in the circumferential and meridian directions ($\partial/\partial\theta = \partial/\partial\varphi = 0$), the shear stresses are equal to zero ($\sigma_{r\theta} = \sigma_{r\varphi} = \sigma_{\theta\varphi} = 0$) and the hoop and meridian stresses are equal to each other ($\sigma_{\theta\theta} = \sigma_{\varphi\varphi}$). By considering these conditions, the equilibrium equations in the circumferential and meridian directions will be satisfied spontaneously. Since each layer is assumed to be homogeneous, the equilibrium equation in the radial direction of each layer can be derived as:

$$\frac{\partial \sigma_{rr}^j}{\partial r_j} + \frac{2}{r_j}\left(\sigma_{rr}^j - \sigma_{\theta\theta}^j\right) = 0 \tag{6}$$

The stress-strain relations for homogeneous material can be written as:

$$\sigma_{rr} = \lambda\left(\varepsilon_{rr} + \varepsilon_{\theta\theta} + \varepsilon_{\varphi\varphi}\right) + 2G\varepsilon_{rr} \tag{7a}$$

$$\sigma_{\theta\theta} = \lambda\left(\varepsilon_{rr} + \varepsilon_{\theta\theta} + \varepsilon_{\varphi\varphi}\right) + 2G\varepsilon_{\theta\theta} \tag{7b}$$

where G is the shear modulus and λ is equal to:

$$\lambda = (\upsilon E)/\left[(1+\upsilon)(1-2\upsilon)\right] = 2\upsilon G/(1-2\upsilon) \tag{8}$$

Due to the symmetry, $u_\theta = u_\varphi = 0$, and the strain-displacement relations in the spherical coordinates reduces to:

$$\varepsilon_{rr} = \partial u_r / \partial r - \alpha\Delta T \tag{9a}$$

$$\varepsilon_{\varphi\varphi} = \varepsilon_{\theta\theta} = u_r / r - \alpha\Delta T \tag{9b}$$

$$\varepsilon_{r\theta} = \varepsilon_{r\varphi} = \varepsilon_{\theta\varphi} = 0 \tag{9c}$$

By substituting Eq. (9) in Eq. (7), the stress components in each layer can be derived with respect to the radial displacement component as:

$$\sigma_{rr}^j = \left(\lambda^j + 2G^j\right)\left(\frac{\partial u_r^j}{\partial r_j} + \frac{u_r^j}{r_j}\delta_1 - \delta_2^j \Delta T^j\right) \tag{10a}$$

$$\sigma_{\theta\theta}^j = \lambda^j \left(\frac{\partial u_r^j}{\partial r_j} + \frac{1}{\upsilon}\frac{u_r^j}{r_j} - \frac{2\delta_2^j}{\delta_1}\Delta T^j\right) \tag{10b}$$

where $\Delta T = \Delta T(r_j)$ is the temperature difference between the temperature of each point (which is obtained from Eq. (2)) and the initial temperature, and δ_1 and δ_2^j are defined as:

$$\delta_1 = 2\upsilon/(1-\upsilon) \tag{11}$$

$$\delta_2^j = (1+\upsilon)\alpha^j/(1-\upsilon) \tag{12}$$

By replacing Eq. (10) into Eq. (6) and using Eq. (2), the equilibrium equation can be derived as a function of radial displacement component:

$$\frac{\partial^2 u_r^j}{\partial r_j^2} + \frac{2}{r_j}\frac{\partial u_r^j}{\partial r_j} - \frac{2}{r_j^2} = \frac{\beta^j}{r_j^2} \tag{13}$$

where

$$\beta^j = -(1+\upsilon)\alpha^j D_1^j/(1-\upsilon) \tag{14}$$

The analytical solution of the Eq. (13) is:

$$u_r^j = A_1^j r_j + A_2^j/r_j^2 - \beta^j/2 \tag{15}$$

in which A_1^j and which A_2^j are unknown coefficients that can be determined by applying the boundary conditions. Due to the presence of viscoelastic interfaces, the radial stress is continuous, while the displacement is not:

$$\sigma_{rr}^j\big|_{r_{j+1}} = \sigma_{rr}^{j+1}\big|_{r_{j+1}}, \quad j=1,\ldots,N-1 \tag{16a}$$

$$u_r^j\big|_{r_{j+1}} = u_r^{j+1}\big|_{r_{j+1}} + \gamma^j, \quad j=1,\ldots,N-1 \tag{16b}$$

In this equation, γ^j denotes the displacement magnitude at the j-th interface and is related to the stress (at this interface) by employing the Kelvin-Voigt viscoelastic model as below:

$$\sigma_{rr}^j = \eta_0^j \gamma^j + \eta_1^j \frac{\partial \gamma^j}{\partial t}, \quad j=1,\ldots,N-1 \tag{17}$$

In this equation, η_0^j and η_1^j are respectively the elastic and viscoelastic constants of the j-th interface. The above relation may be rewritten in the dimensionless form as:

$$\frac{h\sigma_{rr}^j}{E_{out}} = \bar{\eta}_0^j \gamma^j + \bar{\eta}_1^j \frac{\partial \gamma^j}{\partial \hat{\delta}}, \quad j=1,\ldots,N-1 \tag{18}$$

in which

$$\tau = E_{out} t/\left(\eta_1^1 h\right) \tag{19}$$

$$\bar{\eta}_0^j = \eta_0^j h/E_{out} \tag{20}$$

$$\bar{\eta}_1^j = \eta_1^j/\eta_1^1 \tag{21}$$

where h denotes the total vessel thickness and E_{out} is the elastic modulus of the outer layer. Eq. (18) is a linear time-dependent differential equation with constant coefficients. By solving this equation, γ^j c may be obtained as follows:

$$\gamma^j = \frac{h\sigma_{rr}^j}{E_{out}\bar{\eta}_0^j}\left(1 - exp\left(-\frac{\bar{\eta}_0^j}{\bar{\eta}_1^j}\tau\right)\right) \tag{22}$$

Based on this equation, γ^j can be determined at each moment and its value can be substituted into Eq. (16b). By repeating Eqs. (16a) and (16b) in (N-1) interfaces, (2N-2) equations will be obtained. In addition, the radial stresses at the inner and outer surfaces are equal to the internal and external pressures, respectively. However, since at the first step only the thermal stresses are considered, the radial stresses at these surfaces are zero. By employing Eq. (10a), these two conditions can be expressed as:

$$\left(\frac{\partial u_r^{\ 1}}{\partial r_1} + \frac{u_r^{\ 1}}{r_1}\delta_1 - \delta_2^{\ 1}\Delta T^1 \right) = 0 \tag{23}$$

$$\left(\frac{\partial u_r^{\ N+2}}{\partial r_{N+2}} + \frac{u_r^{\ N+2}}{r_{N+2}}\delta_1 - \delta_2^{\ N+2}\Delta T^{N+2} \right) = 0 \tag{24}$$

These two equations along with (2N-2) previous equations will result in 2N equations. Meanwhile, according to Eq. (15), there are two unknown coefficients for each layer ($A_1^{\ j}$ and $A_2^{\ j}$). Therefore, for a number of N layers, there will be 2N unknown coefficients at hand. This procedure creates a linear set of equations with 2N equations and 2N unknowns. The solution to this set of equations gives $A_1^{\ j}$ and $A_2^{\ j}$ for all layers. By determining these two coefficients, the stress and displacement fields can be obtained for each layer and consequently for the whole vessel.

2- 2- Mechanical loading
In the second step, the induced mechanical stress field, produced by the internal and external pressures is determined by taking into account the effects of the viscoelastic interfaces. The equation of equilibrium and the stress-strain relations are the same as Eqs. (6) and (7) that can be simplified as

$$\varepsilon_{rr} = \partial u_r / \partial r \tag{25a}$$

$$\varepsilon_{\varphi\varphi} = \varepsilon_{\theta\theta} = u_r / r \tag{25b}$$

$$\varepsilon_{r\theta} = \varepsilon_{r\varphi} = \varepsilon_{\theta\varphi} = 0 \tag{25c}$$

By substituting the above equations into the stress-strain relations of each layer, the stress components can be obtained as a function of radial displacement:

$$\sigma_{rr}^{\ j} = \left(\lambda^j + 2G^j \right)\left(\frac{\partial u_r^{\ j}}{\partial r_j} + \frac{u_r^{\ j}}{r_j}\delta_1 \right) \tag{26a}$$

$$\sigma_{\theta\theta}^{\ j} = \lambda^j \left(\frac{\partial u_r^{\ j}}{\partial r_j} + \frac{1}{\upsilon}\frac{u_r^{\ j}}{r_j} \right) \tag{25b}$$

Substituting Eq. (25) into Eq. (6) will present the equation of equilibrium for each layer as:

$$\frac{\partial^2 u_r^{\ j}}{\partial r_j^{\ 2}} + \frac{2}{r_j}\frac{\partial u_r^{\ j}}{\partial r_j} - \frac{2}{r_j^{\ 2}} = 0 \tag{27}$$

which solution is

$$u_r^{\ j} = B_1^{\ j} r_j + B_2^{\ j} / r_j^{\ 2} \tag{28}$$

where, $B_1^{\ j}$ and $B_2^{\ j}$ are unknown coefficients and can be determined by means of boundary conditions. The interfacial boundary conditions are similar to the previous step and can be expressed as Eq. (16). However, the boundary conditions at the inner and outer surfaces are different from Eqs. (23) and (24); since the internal and the external pressures should be

considered as the radial stresses at these surfaces, respectively. Thus, the boundary conditions at these two surfaces can be written as:

$$\left(\lambda^1 + 2G^1 \right)\left(\frac{\partial u_r^{\ 1}}{\partial r_1} + \frac{u_r^{\ 1}}{r_1}\delta_1 \right) = P_{in} \tag{29}$$

$$\left(\lambda^{N+2} + 2G^{N+2} \right)\left(\frac{\partial u_r^{\ N+2}}{\partial r_{N+2}} + \frac{u_r^{\ N+2}}{r_{N+2}}\delta_1 \right) = P_{out} \tag{30}$$

Repeating Eqs. (16a) and (16b) for (N-1) interfaces along with Eqs. (29) and (30) will produce 2N equations. On the other hand, there are two unknown coefficients for each layer that means a number of 2N unknown coefficients exist for the whole vessel. Therefore, there exist a linear set of 2N equations with 2N unknowns. The solution to this set determines the displacement field from which the stress field may be calculated. The final displacement and stress fields are obtained by the summation of the corresponding thermal and mechanical fields. It should be mentioned that the equations are coded in MAPLE software and the results are acquired.

3- Results and Discussion
As there are almost no other studies on the spherical vessels with viscoelastic interface of layers, a spherical vessel with perfect interfaces (in which the displacement is continuous in the interfaces and γ^j=0) is assumed to verify the developed solution method. In order to investigate the validity of the present model, an FG vessel with similar loading condition is employed which has been already studied by Eslami et al. [5]. They have considered the inner and outer radii of the FG vessel equal to 1 m and 1.2 m, respectively. Also, at the inner and outer surfaces, the temperature is 10 ºC and 0 ºC, respectively, and the internal pressure is assumed equal to 50 MPa. The changes in the thermal and mechanical properties of the vessel are expressed by power law as:

$$E = E_{in}r^n \tag{31}$$

$$\alpha = \alpha_{in}r^n \tag{32}$$

where, E_{in} and α_{in} denote the elastic modulus and thermal expansion coefficient of the inner surface and are assumed to be equal to 200 GPa and 1.2×10^{-6} 1/K , respectively. Fig. 2 shows a comparison between the obtained temperature distribution, displacement and radial stress by the present model and the results presented by Eslami et al. [5]. As can be seen in this figure, a good agreement is obtained between the mentioned results which shows the validity and accuracy of the present model. Here, again, it should be emphasized that the present model can also predict the thermo-mechanical behavior of a functionally graded spherical vessel with continuous variation of mechanical and thermal properties.

After verifying, the present model is used to investigate the effects of different parameters on the thermo-mechanical behavior of the spherical layered vessel with viscoelastic interfaces. In order to investigate the effects of several parameters, the spherical vessel is assumed to have ten homogeneous layers, varying from a ceramic inner layer to a metallic outer layer. Therefore, the spherical vessel contains ten homogeneous layers with imperfect viscoelastic interfaces between them. Table 1 lists the thermal and mechanical properties of the ceramic and metallic layers used to produce

(a)

(b)

(c)
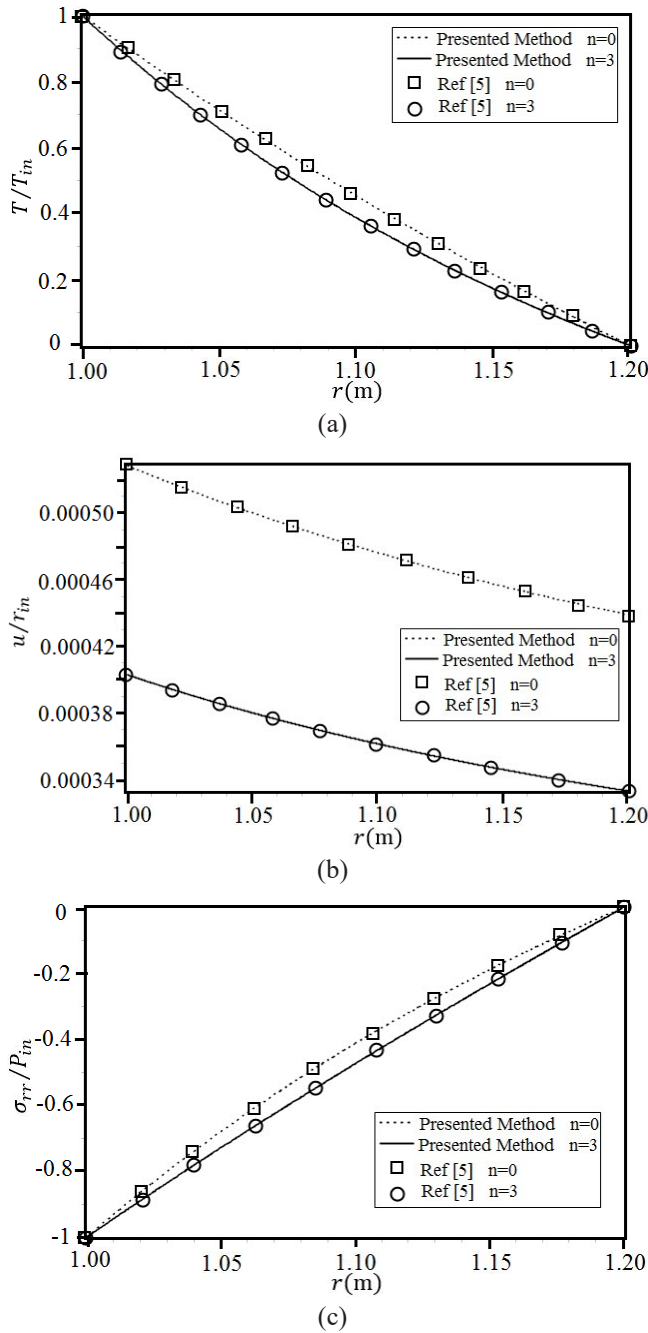
Fig. 2. Comparison between the obtained results by the present model and the results of Eslami et al. [5]; (a) Temperature distribution through the vessel thickness, (b) Dimensionless displacement; (c) Dimensionless radial stress

numerical results. The viscoelastic interfaces are assumed to be the same between each two adjacent layers. In addition, the thickness of these layers is assumed to be negligible and the thermo-mechanical properties are considered to be $\overline{\eta}_0=0.05$ and $\overline{\eta}_1=1$.

Table 1. Thermal and mechanical properties of the ceramic and metallic layers

Material	$\alpha \ [10^{-6}/\text{K}]$	k [W/m.K]	E [GPa]
Steel (metallic component)	200	17	13.2
Glass coating (ceramic component)	70	1	0.65

The inner and outer radii of the vessel are 1 m and 1.2 m, respectively. The initial temperature of the whole vessel is assumed to be 25 ºC. Heat convection is assumed at both inner and outer surfaces of the vessel where heat transfer coefficient is considered to be equal to 10 W/(m².K); and the inner and outer fluid temperatures ($T_{\infty_{in}}$ and $T_{\infty_{out}}$) are assumed to be 150 ºC and 25 ºC, respectively. After the temperature reaches a steady-state condition, the vessel is subjected to an internal pressure of 50 MPa, while no external pressure is applied. Here, the effects of different parameters are discussed, while the other parameters are considered to be constant. In all of the following investigations, the radial displacement and stress are non-dimensionalized with respect to the total thickness and the internal pressure of the vessel, respectively.

3- 1- The effect of time

As mentioned earlier, the presence of the viscoelastic interfaces between the layers leads to a time-dependent response of the system, even under static loading conditions. Since the heat transfer equation is solved in the steady-state situation, the instantaneous temperature distribution cannot be obtained. Therefore, the problem is defined in a way that at first the vessel is subjected to the described thermal loading and after the temperature distribution in the vessel reaches a steady-state condition, the mechanical loading in the form of internal pressure is applied. After applying the internal pressure, the response of the system can be achieved at each time meaning that the time-dependent behavior of the vessel can be obtained.

Fig. 3 demonstrates the vessel time history response to the mechanical load. In this case, the thermal load is not inserted and only an internal pressure of 50 MPa is applied. As can be seen in Fig. 3a, due to the presence of the viscoelastic interfaces, the radial displacement varies with time. In other words, right after the vessel is subjected to the internal pressure, its layers tend to expand; while the viscoelastic interfaces cannot be expanded in a synchronized manner. As time goes on, this displacement reaches a stable state. In such a state, for $\tau>100$ no changes occur in the diagrams. When the response of the system reaches the steady-state, the displacement discontinuity can be noticeably seen between any adjacent layers. Furthermore, the variation of radial stress versus time can be seen in Fig. 3b. In addition, it can be seen that in the beginning moment of inserting the internal pressure, the radial stress varies linearly through the thickness of the vessel, while it decreases as time passes and reaches the steady-state.

3- 2- The effect of internal pressure

Figs. 4 and 5 illustrate the time history of the response of the vessel subjected to an internal pressure of 5 MPa and 500 MPa, respectively. In both these figures, the thermal loading is neglected in order to only investigate the effect of mechanical loading. By comparing these diagrams with those of Fig. 3, it can be concluded that the internal pressure variation does not affect the stabilization time of the system. In addition, it can be seen that the displacement and stress vary linearly versus the internal pressure. Thus, the non-dimensional stress (σ_{rr}/P_{in}) has remained the same in all these three figures; but the non-dimensional displacement (*u*/h) varies linearly versus pressure.

(a)

(b)
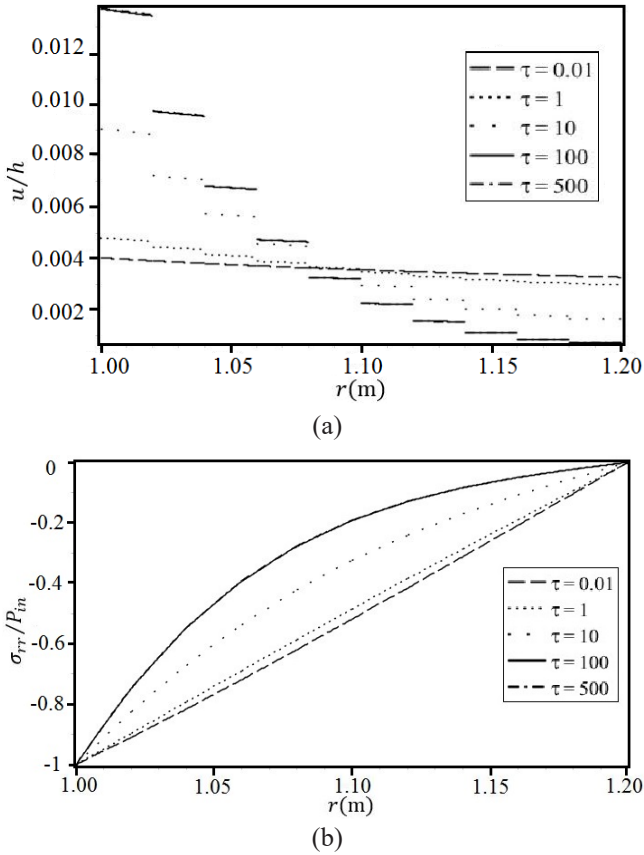
Fig. 3. The response of the system for the internal pressure of 50 MPa with no thermal loading; (a) Non-dimensional radial displacement, (b) Non-dimensional radial stress

(a)

(b)

Fig. 4. The response of the system for the internal pressure of 5 MPa with no thermal loading; (a) Non-dimensional radial displacement, (b) Non-dimensional radial stress

(a)

(b)

Fig. 5. The response of the system for the internal pressure of 500 MPa with no thermal loading; (a) Non-dimensional radial displacement, (b) Non-dimensional radial stress

3- 3- The effect of thermal loading

In this section, the internal pressure is assumed to be equal to zero, in order to study the effect of thermal loading. The results are presented for the steady-state conditions, where the temperature distribution has reached to its steady condition.

Fig. 6 demonstrates the temperature distribution through the wall of the vessel for different temperatures of the inner fluid, and Fig. 7 depicts the displacement and stress due to this temperature distribution. As can be seen in these two figures, if the internal temperature is less than the initial temperature, the overall temperature decreases and the vessel tends to shrink. On the other hand, since the thermal expansion coefficient of the metal is higher than the ceramic (Table 1), the outer metal richer layers have a greater tendency to shrink, and therefore the inner layers will be compressed. If
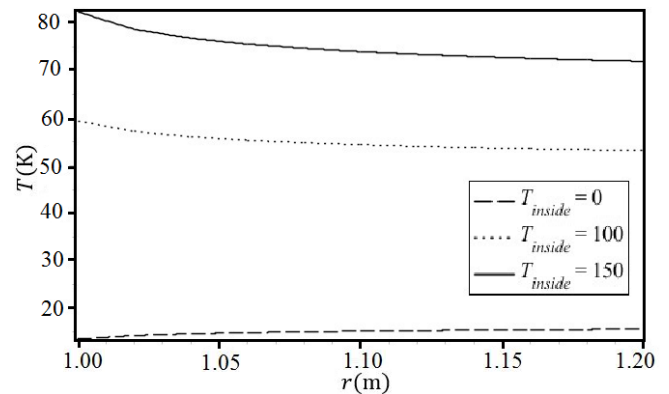
Fig. 6. Temperature distribution through the wall of the vessel for different inner fluid temperatures

81

the internal temperature is higher than the initial temperature, the temperature increases in all layers and the vessel tends to expand. Because the outer layers expand more than the inner layers, tensile stresses will be produced in all layers.

(a)

(b)
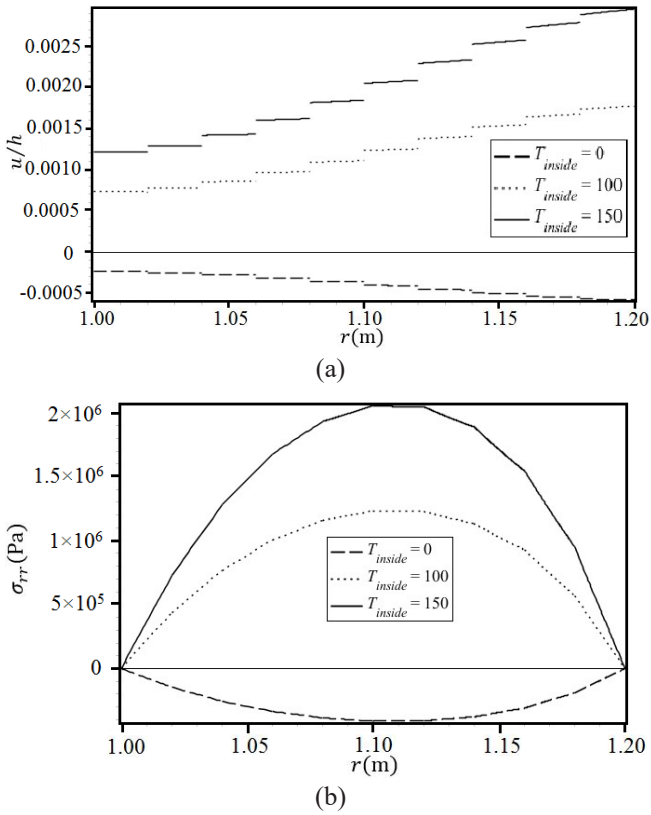
Fig. 7. (a) Non-dimensional displacement and (b) radial stress due to different thermal loadings

3- 4- The effects of thermal and loading conditions

In this section, by means of the superposition principle, the simultaneous effects of thermal and mechanical loadings on the behavior of the spherical vessel are investigated. By determining the displacement and stress fields caused by the thermal and mechanical loadings, the response of the system to any thermo-mechanical loading can be easily predicted.

Fig. 8 illustrates the induced displacement and stress by an internal pressure of 50 MPa and an inner fluid temperature of 150 ºC. As can be seen in the figure, the effect of the internal pressure is dominant in the inner layers, while in the outer layers, where the effect of mechanical stress decreases, the effect of thermal stress is dominant. This is due to the fact that according to the results of the previous sections, a maximum stress of 2 MPa is produced because of the thermal loading for an inner fluid temperature of 150 ºC which has been the maximum inner fluid temperature. Meanwhile, the stress produced by the mechanical loading is in the order of applied internal pressure that is much higher than the thermal stress. By increasing the internal pressure, the effect of mechanical stress becomes more dominant than the thermal stress and the behavior of the vessel gets closer to Fig. 3.

(a)

(b)
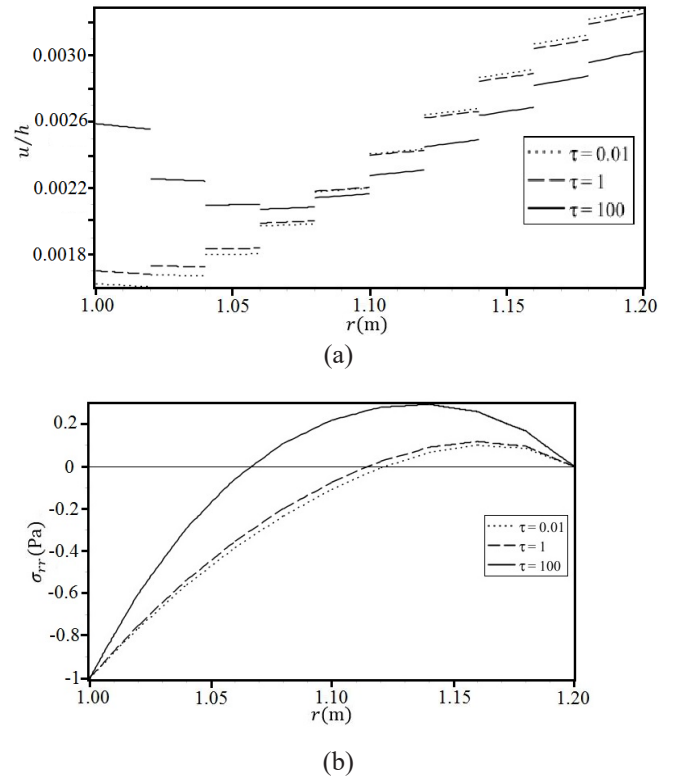
Fig. 8. The response of the system for the internal pressure of 500 MPa and the inner fluid temperature of 150 ºC; (a) Non-dimensional radial displacement, (b) Non-dimensional radial stress

3- 5- The effect of $\bar{\eta}_0$ and $\bar{\eta}_1$

Different cases are studied in order to investigate the effects of the parameters of the viscoelastic layer. In the first case, it is assumed that all interfaces possess the same properties and only the effect of $\bar{\eta}_0$ is discussed. For this purpose, $\bar{\eta}_1^j$ ($j=1,\ldots,(N-1)$) is considered equal to unity and the behavior of the vessel under thermal and mechanical loadings is studied for three different values of $\bar{\eta}_0^j$. Fig. 9 demonstrates the effect of this parameter on the non-dimensional displacement. It can be concluded from this figure that by increasing the value of $\bar{\eta}_0^j$, the stabilization time of the system decreases. In other words, higher values of $\bar{\eta}_0^j$ means stiffer viscoelastic layers which leads to a reduction in the displacement of these layers and consequently overall displacement of the wall of the vessel. This may be explained by Eq. (22), as well.

(a)

(b)

(b)

(c)

(c)
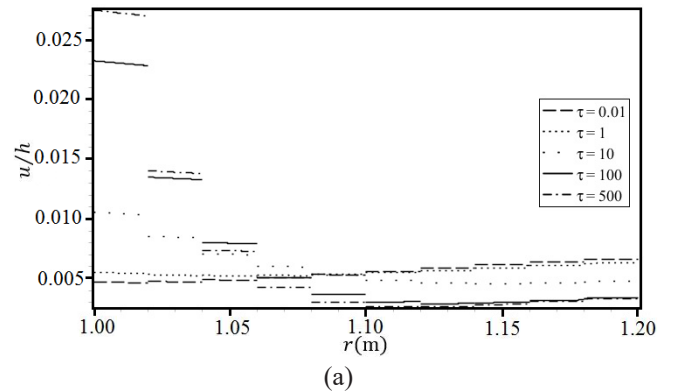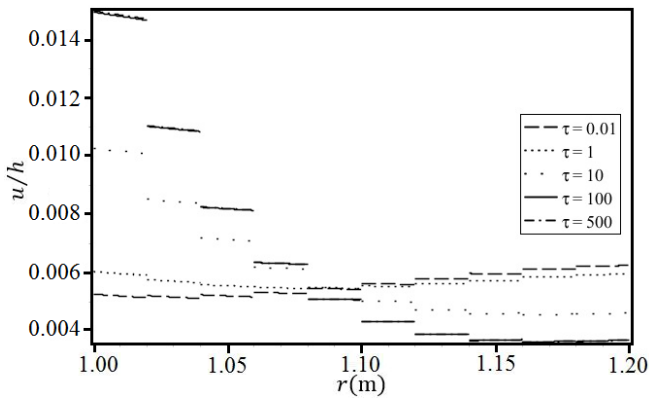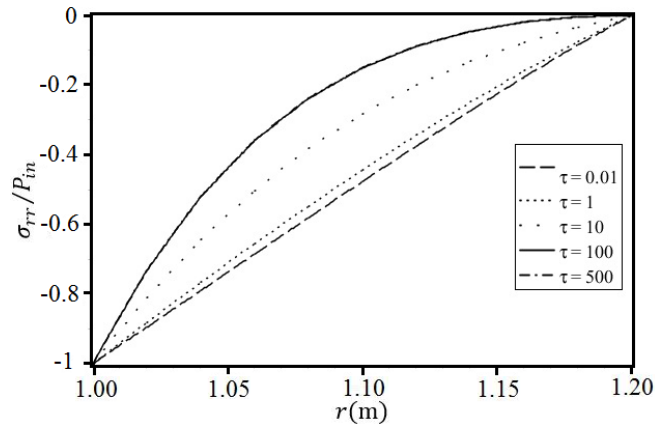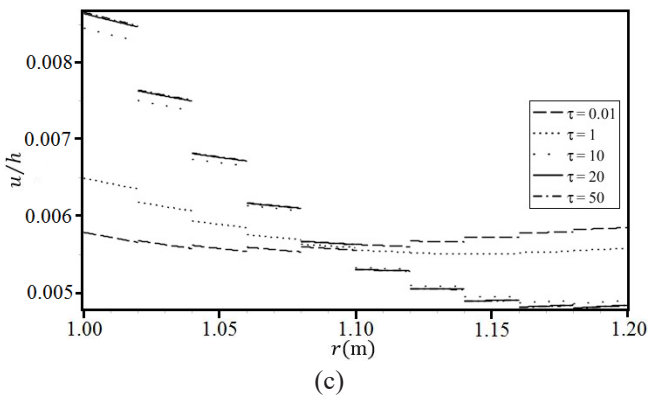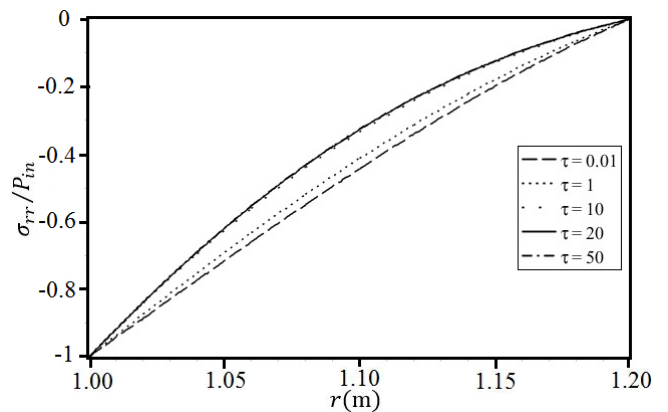
Fig. 9. The effect of $\bar{\eta}_0^j$ on the non-dimensional displacement of the spherical vessel under mechanical and thermal loadings, (a) $\bar{\eta}_0^j$=0.01, (b) $\bar{\eta}_0^j$=0.05 and (c) $\bar{\eta}_0^j$=0.25

Fig. 10 depicts the non-dimensional stress distribution along the vessel thickness. According to this figure, by increasing the value of $\bar{\eta}_0^j$, the stiffness of the viscoelastic layer increases, which in turn increases the value of the stress in different layers. This is due to the fact that if the viscoelastic layer possesses a lower stiffness, it can endure higher stresses through higher deformations, which reduces the stress in other layers of the vessel. In other words, when $\bar{\eta}_0^j$ increases, the viscoelastic layer becomes stiffer and thus deforms less and this less deformation passes the stress to the other layers. In the second case, various viscoelastic parameters are considered for different layers. In order to investigate the effect of changing $\bar{\eta}_0^j$ of only one layer, this parameter is changed in that specific layer and all other $\bar{\eta}_0^j$ are kept

Fig. 10. The effect of $\bar{\eta}_0^j$ on the non-dimensional stress of the spherical vessel under mechanical and thermal loadings, (a) $\bar{\eta}_0^j$=0.01, (b) $\bar{\eta}_0^j$=0.05 and (c) $\bar{\eta}_0^j$=0.25

constant and equal to 0.05 and $\bar{\eta}_1^j$=1. Fig. 11 illustrates the effect of variation of $\bar{\eta}_0$ in one interface on the non-dimensional displacement of the whole vessel.

By comparing the results presented in this figure with the results of Fig. 9b (where $\bar{\eta}_0^j$=0.05 for all interfaces), it can be concluded that by changing the value of $\bar{\eta}_0$ even in one interface, the stabilization time of the system and the also ultimate displacement of all layers change. However, the effect of changing this parameter is not the same for each interface and by approaching to the outer layers (as j increases in $\bar{\eta}_0^j$), this effect decreases. For example, by decreasing the amount of $\bar{\eta}_0^1$ from 0.05 to 0.01, the displacement of the first layer increases about 60%; while by decreasing the value

(a)

(a)

(b)

(b)
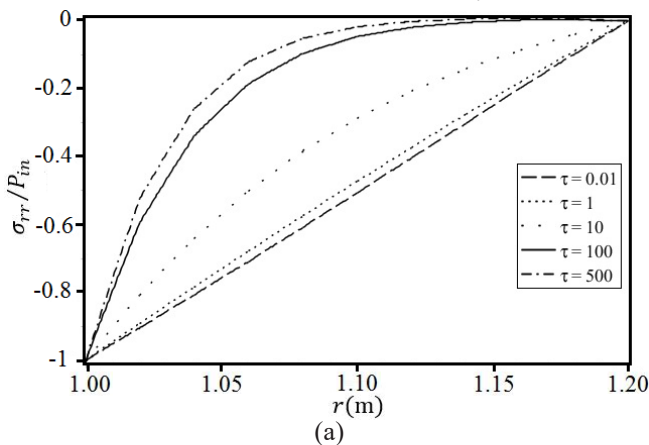
(c)
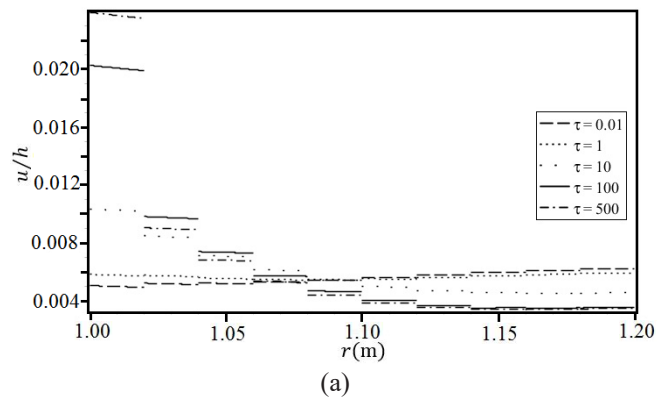
(c)
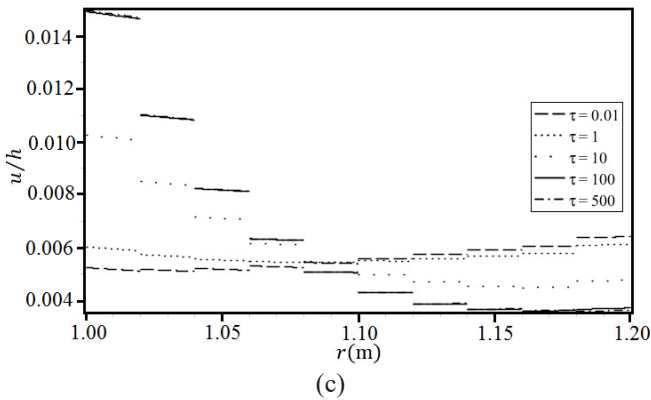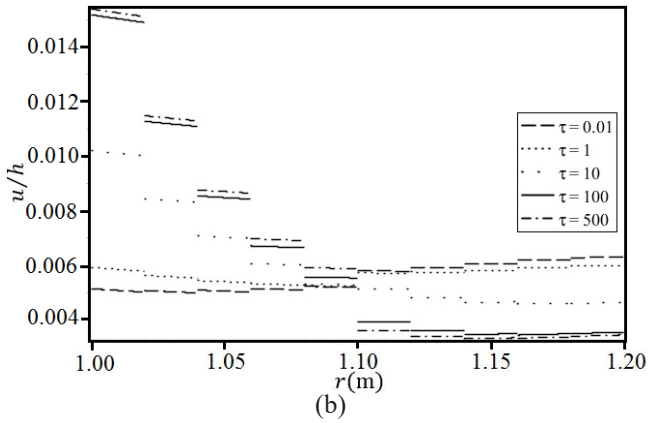
Fig. 11. The effect of changing of $\bar{\eta}_0^j$ in one of the interfaces on the non-dimensional displacement of the spherical vessel under thermal and mechanical loadings; (a) $\bar{\eta}_0^1$=0.01 and $\bar{\eta}_0^j$=0.05 for all other interfaces, (b) $\bar{\eta}_0^5$=0.01 and $\bar{\eta}_0^j$=0.05 for all other interfaces and (c) $\bar{\eta}_0^9$=0.01 and $\bar{\eta}_0^j$=0.05 for all other interfaces

Fig. 12. The effect of changing of $\bar{\eta}_0^j$ in each interface on the non-dimensional stabilized displacement of the spherical vessel under thermal and mechanical loadings. (a) the effect of changing $\bar{\eta}_0^1$; (b) the effect of changing $\bar{\eta}_0^5$; (c) the effect of changing $\bar{\eta}_0^9$

of $\bar{\eta}_0^5$ from 0.05 to 0.01, only a 3% increase occurs in the displacement of the first layer, and by decreasing the value of $\bar{\eta}_0^9$ only negligible changes occur in the displacement of the first layer. This is due to the fact that the amount of the stabilized displacement of the inner layers is much greater than that of the stabilized displacement of outer layers, and therefore, the response of the system is more sensitive to the properties of the inner layers rather than the outer layers. This description is also shown in Fig. 12.

Fig. 13 shows the effect of changing the value of $\bar{\eta}_0^j$ in only one of the interfaces on the stabilized stress of the whole thickness. The results show that, by changing the value of $\bar{\eta}_0^j$ in one of the interfaces, the produced stress in the whole vessel changes in such a manner whose effect is more
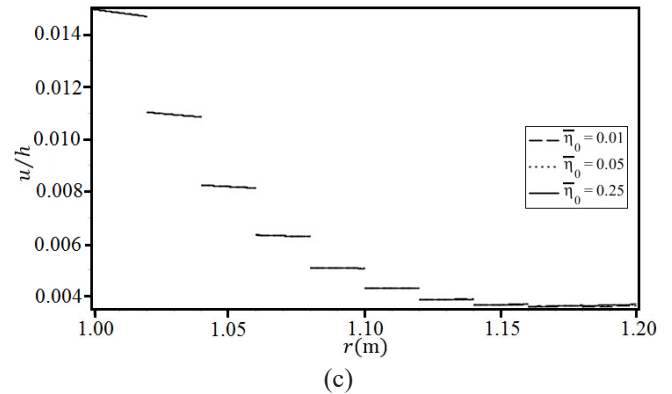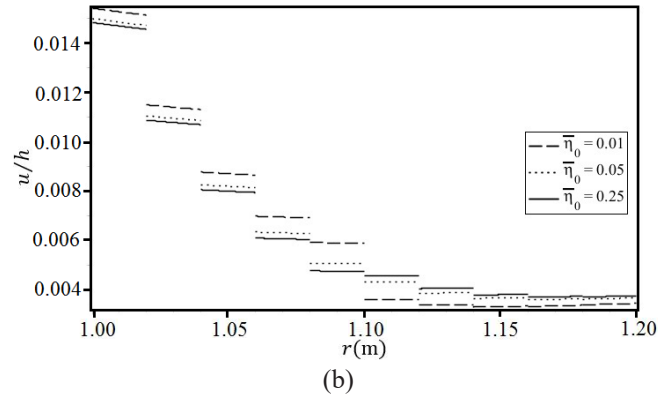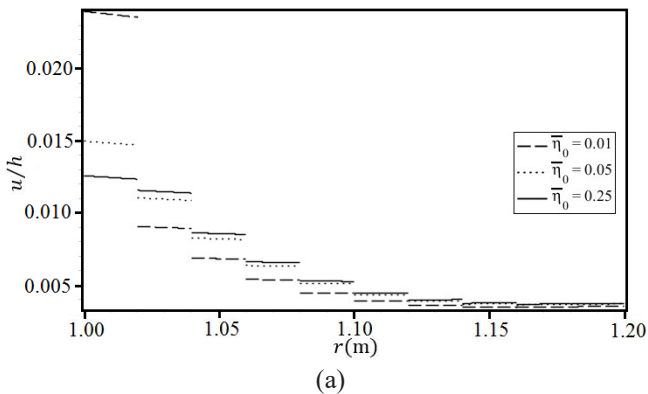
significant on the outer layers rather than the inner ones. Meanwhile, the effect of changing of $\bar{\eta}_0^j$ is not the same for different interfaces and by approaching to the outer layers, this effect vanishes.

(a)

(a)

(b)

(c)
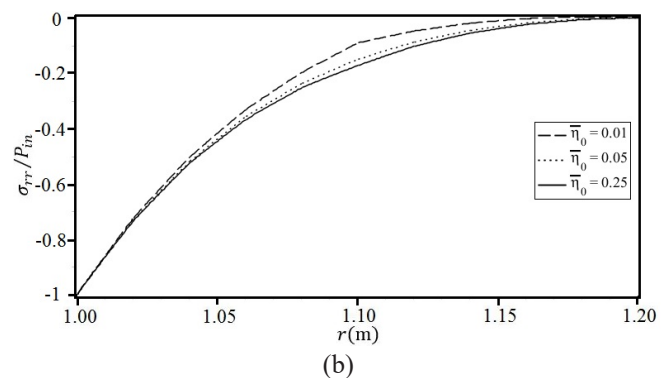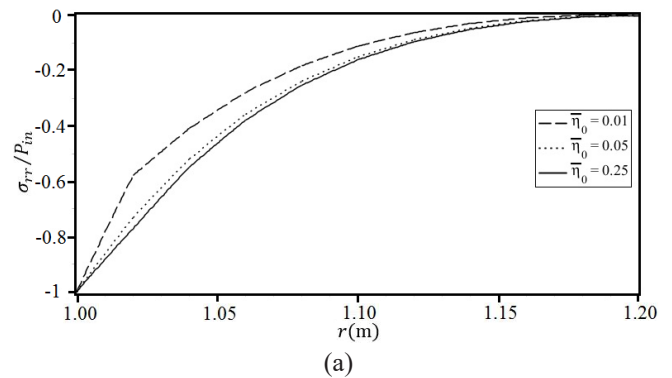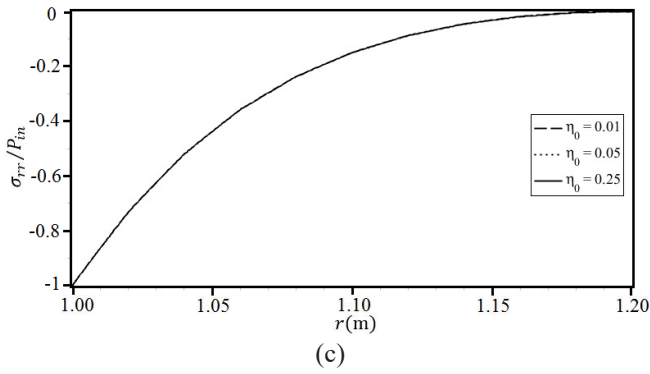
Fig. 13. The effect of changing of $\bar{\eta}_0^j$ in each interface on the non-dimensional stabilized stress of the spherical vessel under thermal and mechanical loadings. (a) the effect of changing $\bar{\eta}_0^1$; (b) the effect of changing $\bar{\eta}_0^5$; (c) the effect of changing $\bar{\eta}_0^9$

In order to study the effect of $\bar{\eta}_1^j$, a case is considered in which $\bar{\eta}_0^j=0.05$, $\bar{\eta}_1^1=1$ and $\bar{\eta}_1^j$ for all other layers are the same and equal to 0.1 and 10. Figs. 14 and 15 demonstrate the effect of $\bar{\eta}_1^j$ on the non-dimensional displacement and stress of the vessel, respectively. Comparing the results of Figs. 14 and 15 with the those of Figs. 9b and 10b (in which $\bar{\eta}_1^j=1$ for all layers), reveals the fact that increasing $\bar{\eta}_1^j=1$ increases the stabilization time of the system while this variation does not affect the amount of the stabilized displacement and stress. This may be explained by considering the fact that $\bar{\eta}_1^j$ is factor which represents the effect of time. As time passes and the system reaches its steady-state, $\bar{\eta}_1^j$ loses its effect and the parameter that controls the displacement and stress is $\bar{\eta}_0^j$. Thus, it may also be concluded by means of Eq. (22).

(a)

(b)
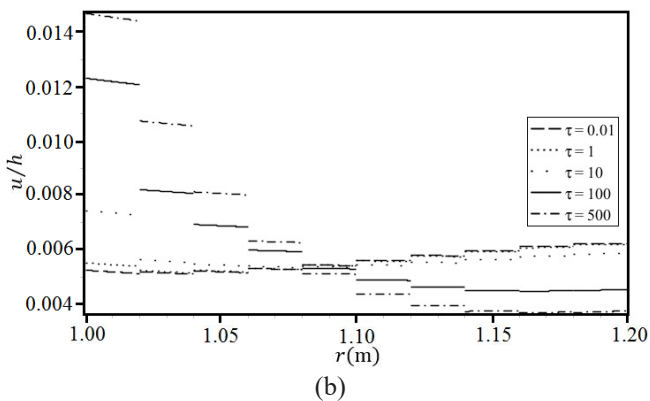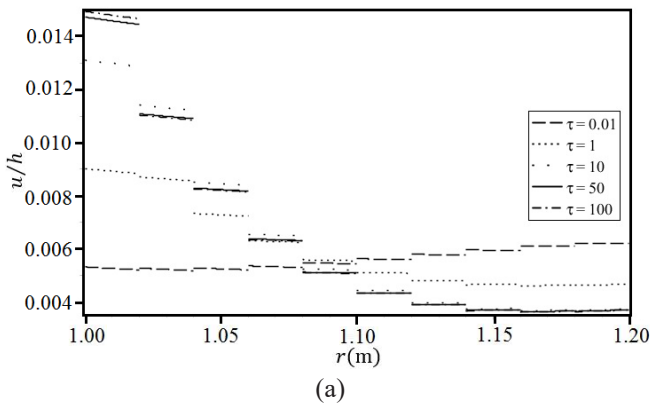
Fig. 14. The effect of changing of $\bar{\eta}_1^j$ on the non-dimensional stabilized displacement of the spherical vessel under thermal and mechanical loadings. (a) $\bar{\eta}_1^1=1$ and $\bar{\eta}_1^j=0.1$ for other interfaces; (b) $\bar{\eta}_1^1=1$ and $\bar{\eta}_1^j=10$ for other interfaces

(a)

(b)
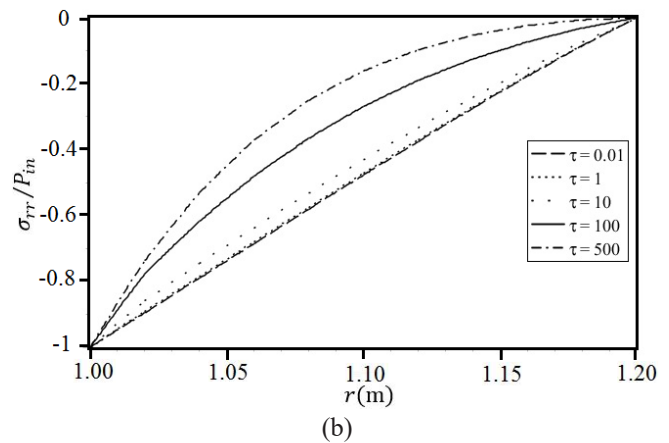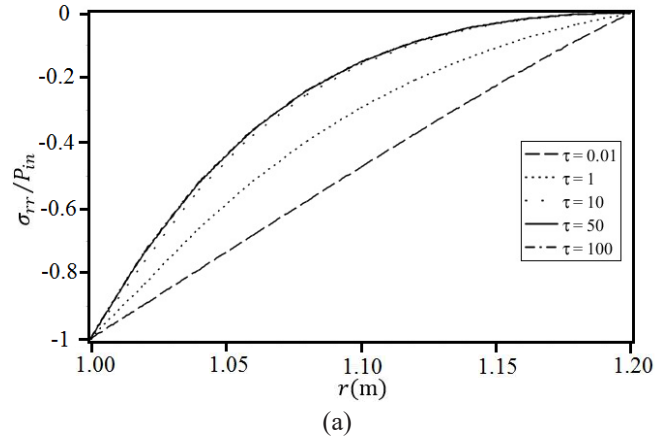
Fig. 15. The effect of changing of $\bar{\eta}_1^j$ on the non-dimensional stabilized stress of the spherical vessel under thermal and mechanical loadings. (a) $\bar{\eta}_1^1=1$ and $\bar{\eta}_1^j=0.1$ for other interfaces; (b) $\bar{\eta}_1^1=1$ and $\bar{\eta}_1^j=10$ for other interfaces

4- Conclusions

In this paper, the time-dependent response of a layered spherical vessel with viscoelastic interfaces of negligible thickness, under thermal and mechanical loadings has been analytically investigated. To this end, the thermoelasticity equations have been solved for each layer and by applying suitable boundary conditions, the displacement and stress fields have been determined through the thickness of the vessel. After verification, the proposed model is employed to determine the effects of different parameters on the response of the system. The obtained results showed that the presence of viscoelastic interfaces leads to a discontinuous displacement field along the wall thickness, while the stress field remains continuous. Furthermore, the presence of viscoelastic interfaces makes the system response time-dependent. Meanwhile, it should be mentioned that the response of the system becomes stable as time goes on. Investigating the effects of different parameters revealed that the only parameters that affect the stabilization time are the parameters of the viscoelastic layers (e.g. $\bar{\eta}_0$ and $\bar{\eta}_1$); while, parameters such as the magnitude of the thermal and mechanical loadings do not affect the stabilization time. Generally, by increasing the magnitude of $\bar{\eta}_0$ and decreasing the magnitude of $\bar{\eta}_1$ the stabilization time decreases. Also, it is shown that changing the magnitude of $\bar{\eta}_0$ can affect the final displacements and stresses in the vessel, while changing the magnitude of $\bar{\eta}_1$ does not change the magnitude of these

fields. In addition, changing the viscoelastic properties of each interface may change the stabilization time of the system and the produced displacements and stresses of other layers, as well. However, changes which are made in the properties of different layers have different effects. The results showed that the displacement and stress fields vary linearly versus the internal pressure of the vessel.

References

[1] N. Noda, Thermal stresses in materials with temperature-dependent properties, *Appl. Mech. Rev*, 44(9) (1991) 383-397.

[2] M.P. Lutz, R.W. Zimmerman, Thermal stresses and effective thermal expansion coefficient of a functionally gradient sphere, *Journal of Thermal stresses*, 19(1) (1996) 39-54.

[3] N. Tutuncu, M. Ozturk, Exact solutions for stresses in functionally graded pressure vessels, *Composites Part B: Engineering*, 32(8) (2001) 683-686.

[4] L. You, J. Zhang, X. You, Elastic analysis of internally pressurized thick-walled spherical pressure vessels of functionally graded materials, *International Journal of Pressure Vessels and Piping*, 82(5) (2005) 347-354.

[5] M. Eslami, M. Babaei, R. Poultangari, Thermal and mechanical stresses in a functionally graded thick sphere, *International Journal of Pressure Vessels and Piping*, 82(7) (2005) 522-527.

[6] R. Poultangari, M. Jabbari, M. Eslami, Functionally graded hollow spheres under non-axisymmetric thermo-mechanical loads, *International Journal of Pressure Vessels and Piping*, 85(5) (2008) 295-305.

[7] T. Akis, Elastoplastic analysis of functionally graded spherical pressure vessels, *Computational Materials Science*, 46(2) (2009) 545-554.

[8] N. Tutuncu, B. Temel, A novel approach to stress analysis of pressurized FGM cylinders, disks and spheres, *Composite Structures*, 91(3) (2009) 385-390.

[9] M. Jabbari, S. Karampour, M. Eslami, Radially symmetric steady state thermal and mechanical stresses of a poro FGM hollow sphere, *ISRN Mechanical Engineering*, 2011 (2011).

[10] M.Z. Nejad, M. Abedi, M.H. Lotfian, M. Ghannad, An exact solution for stresses and displacements of pressurized FGM thick-walled spherical shells with exponential-varying properties, *Journal of Mechanical Science and Technology*, 26(12) (2012) 4081-4087.

[11] Y. Bayat, M. Ghannad, H. Torabi, Analytical and numerical analysis for the FGM thick sphere under combined pressure and temperature loading, *Archive of Applied Mechanics*, 82(2) (2012) 229-242.

[12] W. Chen, J. Cai, G. Ye, Exact solutions of cross-ply laminates with bonding imperfections, *AIAA journal*, 41(11) (2003) 2244-2250.

[13] W. Chen, K.Y. Lee, Three-dimensional exact analysis of angle-ply laminates in cylindrical bending with interfacial damage via state-space method, *Composite Structures*, 64(3) (2004) 275-283.

[14] A. Chakrabarti, P. Topdar, A.H. Sheikh, Vibration and buckling of laminated sandwich plates having interfacial imperfections, *European Journal of Mechanics-A/Solids*, 25(6) (2006) 981-995.

[15] Y. Zhou, W. Chen, C. Lü, Semi-analytical solution for orthotropic piezoelectric laminates in cylindrical bending with interfacial imperfections, *Composite Structures*, 92(4) (2010) 1009-1018.

[16] S. Kapuria, P.G. Nair, Exact three-dimensional piezothermoelasticity solution for dynamics of rectangular cross-ply hybrid plates featuring interlaminar bonding imperfections, *Composites Science and Technology*, 70(5) (2010) 752-762.

[17] D.-h. Li, J.-x. Xu, G.-h. Qing, Free vibration analysis and eigenvalues sensitivity analysis for the composite laminates with interfacial imperfection, *Composites Part B: Engineering*, 42(6) (2011) 1588-1595.

[18] D. Li, Y. Liu, Three-dimensional semi-analytical model for the static response and sensitivity analysis of the composite stiffened laminated plate with interfacial imperfections, *Composite Structures*, 94(6) (2012) 1943-1958.

[19] Z. Hashin, Composite materials with viscoelastic interphase: creep and relaxation, *Mechanics of Materials*, 11(2) (1991) 135-148.

[20] H. Fan, G. Wang, Interaction between a screw dislocation and viscoelastic interfaces, *International Journal of Solids and Structures*, 40(4) (2003) 763-776.

[21] L. He, J. Jiang, Transient mechanical response of laminated elastic strips with viscous interfaces in cylindrical bending, *Composites Science and Technology*, 63(6) (2003) 821-828.

[22] W. Chen, K.Y. Lee, Time-dependent behaviors of angle-ply laminates with viscous interfaces in cylindrical bending, *European Journal of Mechanics-A/Solids*, 23(2) (2004) 235-245.

[23] W. Yan, W.-q. Chen, Time-dependent response of laminated isotropic strips with viscoelastic interfaces, *Journal of Zhejiang University-Science A*, 5(11) (2004) 1318-1321.

[24] N.J. Pagano, Exact Solutions for Composite Laminates in Cylindrical Bending, *Journal of Composite Materials*, 3(3) (1969) 398-411.

[25] N.J. Pagano, Influence of Shear Coupling in Cylindrical. Bending of Anisotropic Laminates, *Journal of Composite Materials*, 4(3) (1970) 330-343.

[26] N.J. Pagano, Exact Solutions for Rectangular Bidirectional Composites and Sandwich Plates, *Journal of Composite Materials*, 4(1) (1970) 20-34.

[27] W. Chen, J. Cai, G. Ye, Responses of cross-ply laminates with viscous interfaces in cylindrical bending, *Computer methods in applied mechanics and engineering*, 194(6) (2005) 823-835.

[28] W. Chen, G.W. Kim, K.Y. Lee, The effect of viscous interfaces on the bending of orthotropic rectangular laminates, *Composite structures*, 67(3) (2005) 323-331.

[29] W. Chen, J.P. Jung, G.W. Kim, K.Y. Lee, Cross-ply laminated cylindrical panels with viscous interfaces subjected to static loading, *European Journal of Mechanics-A/Solids*, 24(5) (2005) 728-739.

[30] W. Yan, J. Ying, W. Chen, The behavior of angle-ply laminated cylindrical shells with viscoelastic interfaces in cylindrical bending, *Composite structures*, 78(4) (2007) 551-559.

[31] W. Yan, J. Ying, W. Chen, Response of laminated adaptive composite beams with viscoelastic interfaces, *Composite structures*, 74(1) (2006) 70-79.

[32] W. Yan, W. Chen, Electro-mechanical response of functionally graded beams with imperfectly integrated surface piezoelectric layers, *Science in China Series G: Physics Mechanics and Astronomy*, 49(5) (2006) 513-525.

[33] Y. Wei, Y. Ji, C. Weiqiu, A three-dimensional solution for laminated orthotropic rectangular plates with viscoelastic interfaces, *Acta Mechanica Solida Sinica*, 19(2) (2006) 181-188.

[34] W. Yan, W. Chen, B. Wang, On time-dependent behavior of cross-ply laminated strips with viscoelastic interfaces, *Applied mathematical modelling*, 31(2) (2007) 381-391.

[35] W. Yan, J. Wang, W. Chen, Cylindrical bending responses of angle-ply piezoelectric laminates with viscoelastic interfaces, *Applied Mathematical Modelling*, 38(24) (2014) 6018-6030.

[36] A. Alibeigloo, Three-dimensional static and free vibration analysis of laminated cylindrical panel with viscoelastic interfaces, *Journal of Composite Materials*, 49(19) (2015) 2415-2430.

[37] A. Alibeigloo, Effect of viscoelastic interface on three-dimensional static and vibration behavior of laminated composite plate, *Composites Part B: Engineering*, 75 (2015) 17-28.